Post-irradiation Decomposition of Sulfanylperoxides and Peroxycyclohexadienethiones formed from Thiyl and Peroxyl Radicals

Brynmor Mile,[a] Christopher C. Rowlands,[a] Philip D. Sillman[a] and Andrew J. Holmes[b]
[a] *School of Chemistry and Applied Chemistry, University of Wales College of Cardiff, PO Box 912, Cardiff, UK CF1 3TB*
[b] *Shell Research Ltd., Thornton Research Centre, PO Box 1, Chester, UK CH1 3SH*

Photolysis of (*E*)-azoisobutane and dialkyl and diaryl disulfides in oxygenated 2-methylbutane at temperatures below 230 K results in a very low photostationary state of peroxyl radical, because of the high efficiency of the mixed termination reaction to form sulfanylperoxide and peroxycyclohexadienethione.

Surprisingly, after photolysis is stopped there is an immediate threefold rise in the peroxyl radical concentration. This post-illumination dark reaction is interpreted and accurately modelled using an algorithm, by assuming an irreversible decomposition of the sulfanylperoxide or peroxycyclohexadienethione to alkoxyl and other radicals. Spin traps have been used to confirm the nature of the radicals involved in many of the proposed reactions and to give a measure of radical concentrations under various experimental conditions. Values of the rate parameters for a number of these reactions have been measured and Arrhenius parameters E_2 = 34 kJ mol^{-1}, A_2 = 10^6 s^{-1}, E_2 = 14 kJ mol^{-1}, A_2 = $10^{2.4}$ s^{-1} determined for the decomposition of phenyl and *tert*-butyl sulfanylperoxides, respectively. The low *A* factor for *tert*-butyl sulfonylperoxide is probably associated with a tight, four-membered ring transition state with a loss of internal rotations about partially formed sulfur–oxygen double bonds and accompanying solvent orientations about the more dipolar S=O bond. The decomposition of the phenyl analogue occurs by scission of O–O links in *para* and *ortho* substituted peroxycyclohexadienethione.

Much of the literature on sulfur-containing antioxidants illustrates the complexity of the mechanisms by which these compounds inhibit the autoxidation of hydrocarbons. A range of sulfur-containing radicals such as thiyls (RS$^{\bullet}$), sulfinyls (RSO$^{\bullet}$) and sulfonyls (RSO$_2^{\bullet}$) are participants, as are products of oxidation such as sulfenic acids (RSOH), sulfoxides (RSOR), sulfones (RSO$_2$R) and sulfur dioxide itself.[1–9] Our own work had demonstrated the chemical and mechanistic subtleties of thiyl reactions with spin traps and even simple sulfur compounds, such as dialkyl or diaryl disulfides.[10,11]

We have recently established that there is an efficient termination reaction between *tert*-butyl peroxyls and alkyl or aryl thiyls,[12] to produce sulfanylperoxides, R'SO$_2$R. These are analogous to alkyl trioxides, R'O$_3$R, which have been identified by previous EPR studies.[13,14] Similar compounds, R'NO$_2$R, have also been implicated as unstable intermediates, in the reaction between peroxyl and aminyl radicals to produce alkoxyl and aminoxyl radicals as final products.[15–17] The trioxides decompose into alkoxyl and peroxyl radicals at temperatures about 240 K when both alkyl groups are tertiary. However, if one alkyl group is primary or secondary, the decomposition occurs at 140 K over a period of minutes.

Here we report our EPR studies of the decomposition of two sulfanylperoxides Bu^{t}SO$_2$Bu^t and PhSO$_2$Bu^t and our analysis of an unusual, though not unique, post-irradiation growth of tertiary peroxyls using a kinetic modelling algorithm. The excellent correlation of experimental growth and decay curves with those computed from a fairly simple mechanistic scheme, has allowed us to estimate the Arrhenius parameters for the decomposition of these two sulfanylperoxides.

Experimental

All spectra were recorded on a Varian E109 X-band spectrometer employing 100 kHz modulation. For experiments below ambient temperatures a modified Oxford Instruments temperature controller was used, the temperature recorded being accurate to within ± 1 K. Oxygen-saturated samples in a quartz 4 mm o.d. sample tube were photolysed in a louvered EPR cavity with unfiltered light from a 1 kW Xenon arc lamp. The light beam was not focussed on the sample tube but bathed the cavity's illumination window. Experimentally a thermocouple inserted into the samples showed minimal temperature rises on exposure to the Xenon light beam. *g*-Values were determined using 2,2-diphenyl-1-picrylhydrazyl (DPPH) (g = 2.0036) as the reference and peroxyl concentrations were determined from a calibration of the spin label, 2,2,6,6-tetramethylpiperidin-1-yloxyl (TEMPO).

Solutions of (PhS)$_2$ (10^{-2} to 4 × 10^{-3} mol dm^{-3}) and 2,2'-azoisobutane (AIB) (5 × 10^{-2} to 5 × 10^{-3} mol dm^{-3}) in oxygenated 2-methylbutane (2MB) were photolysed over the temperature range 212–240 K for 5 (kinetic runs) to 40 min and the peroxyl levels monitored during photolysis and for periods of *ca.* 10 min after cessation of photolysis. In the kinetic studies, reactant concentrations were assumed to be constant.

Similar procedures were followed during and after photolysis of oxygenated 2MB solutions of (Bu^{t}S)$_2$ (10^{-1} mol dm^{-3}) and AIB (5 × 10^{-2} mol dm^{-3}), over the temperature range 177–202 K.

In order to establish the types of transient radical present, 5,5-dimethyl-1-pyrroline *N*-oxide (DMPO) (2.5 × 10^{-2} mol dm^{-3}) was added before and after photolysis to oxygenated solutions of AIB (5 × 10^{-2} mol dm^{-3}) and (PhS)$_2$ (5 × 10^{-3} mol dm^{-3}) at 218 K.

The decay characteristics of the peroxyl radicals in the absence and presence of disulfides were determined in separate experiments by photolysing oxygenated solutions of AIB (5 × 10^{-2} mol dm^{-3}), over the temperature range 179–245 K, until a steady state of peroxyl radicals was obtained, and monitoring the decay after the end of photolysis. The effects of

AIB on the rate and order of the peroxyl decay were also determined by varying the AIB concentration (2.5×10^{-2} to 2×10^{-1} mol dm^{-3}).

The growth and decay of peroxyls cannot be solved analytically but could be modelled by numerical methods using an algorithm for solving stiff differential rate equations.

$(PhS)_2$ and $(Bu^tS)_2$ were commercially available samples (Aldrich). AIB (98% purity) was purchased from Lancaster. DMPO and 2MB (HPLC grade) were obtained from Aldrich.

Results and Discussion

The Dark Reaction.—Photolysis of oxygenated 2-methylbutane solutions of AIB at temperatures below 230 K resulted in the formation of tertiary peroxyl radicals (g = 2.015).

$$Bu^{t\bullet} + O_2 \longrightarrow Bu^tO_2^\bullet$$

Addition of phenyl disulfide (10^{-3}–10^{-2} mol dm^{-3}) before photolysis resulted in a marked lowering of the steady-state concentration of peroxyls. A similar but smaller reduction occurred for dialkyl disulfides at the same concentrations. However, surprisingly, on cessation of photolysis, the concentration of peroxyl immediately increased to a plateau value over a period of several minutes and then slowly decayed. Upon resumption of photolysis at any stage the concentration of peroxyl returned to its previous lower value. This cycle of growth and decay and rapid depletion on rephotolysing was repeatable for several cycles (up to seven) with the plateau concentration depleting only slowly with each cycle. This unusual phenomenon is reminiscent of similar behaviour reported for *tert*-butyl methyl trioxide in cyclopropane at 140 K.[14] Such a trioxide is unlikely to be the source of the growth of the tertiary peroxyl in our studies because of the much higher temperatures employed and the fact that no regrowth was observed in the absence of disulfides. Similar regrowth was also observed by using di-*tert*-butyl ketone (TDBK) (10^{-2} mol dm^{-3}) as the photolytic source of *tert*-butyl radicals in the presence of $(Bu^tS_2)_2$ (10^{-1} mol dm^{-3}) in 2-methylbutane. Thus, another possible cause of the regrowth of peroxyl, the photoisomerization of (*E*)-AIB to (*Z*)-AIB and then thermolysis of (*Z*)-AIB,[18–20] can also be discounted.

An important difference between the present experiments and those reported previously[18,20] is the use of a Xenon arc lamp rather than the medium-pressure mercury lamp used in the earlier work. The latter experiments have their highest intensity in the 365 nm region, with only smaller intensities at lower wavelengths. The Xenon lamp has a continuum of radiation from 250 to 1100 nm and a much higher intensity of light below 300 nm. These much higher energy photons here give rise to much more efficient direct photolysis of the AIB to *tert*-butyl radicals and less production *via* the isomerization/thermolysis route. In this context, it is of interest to note that, in our studies, the decay of peroxyl showed good second-order kinetics, in contrast with that observed by Bennett *et al.*[19] who found marked departures from second-order behaviour under conditions where the isomerization/thermolysis reaction occurred. Significantly, a high-pressure mercury lamp was used in this work.[19] We propose that the post-irradiation growth results from the slow thermal decomposition of the sulfanylperoxide, R'SOOR (**1**), produced by the reaction of thiyl with peroxyl radicals (Scheme 1). Both these sulfanylperoxides can decompose by homolytic fission of the weak O–O bond to generate an alkoxyl and sulfinyl radical.* This decomposition is analogous to the decomposition by fission of similar weak O–O bonds in trioxides,[14] tertiary hydroperoxides[21] and the intermediate produced by the reaction of tertiary peroxyls with aromatic aminyl radicals.[15–17] The alkoxyl radicals can subsequently attack the 2-methylbutane solvent cage or diffuse into and then react with bulk solvent to produce mainly the tertiary solvent radicals,[22] which are then rapidly converted into peroxyls. The sulfinyl radicals are unreactive[23] and are rapidly removed by a self-termination reaction. These were not observed because of their resulting low steady-state concentration.

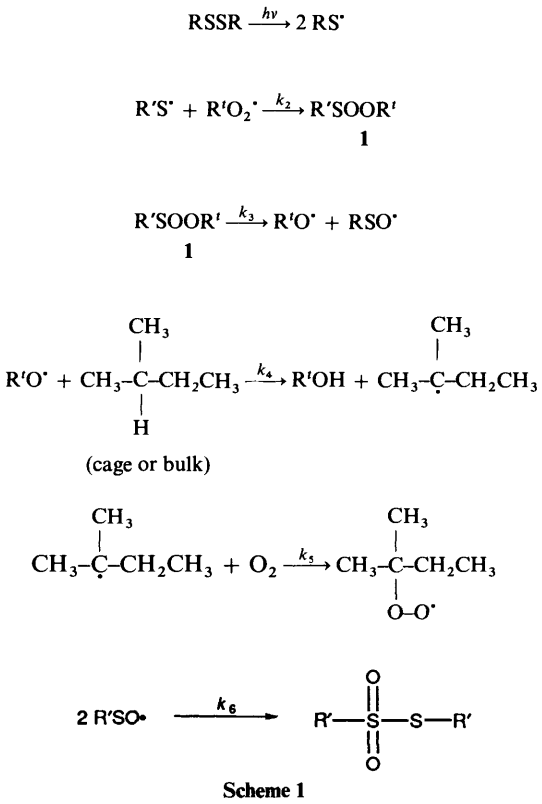

Scheme 1

During photolysis the decomposition of the sulfanylperoxide merely recycles tertiary peroxyl radicals back into the system, where they are rapidly removed by their reaction with thiyls which are continuously produced photolytically, so that only low levels of tertiary peroxyls obtain. However, after photolysis ceases, no thiyls are produced and their concentration quickly falls to very low levels. Thus, the efficient termination reaction of thiyls with peroxyls is eliminated and the tertiary peroxyls are now only removed by the comparatively inefficient self-termination reaction and, hence, their concentration grows to a new higher maximum concentration followed by a slower decay. This maximum concentration is governed by a balance between radical generation from the sulfanylperoxide and radical loss by mutual termination of the peroxyls.

Support for this explanation comes from the following experimental findings.

(*i*) *Effect of irradiation time.* Increasing the photolysis time of solutions of AIB and $(PhS)_2$ resulted in a more extensive regrowth and a higher plateau concentration of peroxyls (Fig. 1) after cessation of photolysis. This was expected since a longer photolysis time would result in a higher net production of sulfanylperoxide.

(*ii*) *Effects of AIB and RSSR concentration.* The extent of regrowth was found to depend critically on the concentration of AIB and disulfide, and on the ratio of their concentrations. For a particular disulfide concentration, there was a maximum

* For phenylthiyl another product, termed a peroxycyclohexadienethione, can also be formed and decomposes by a different mechanism which is discussed later.

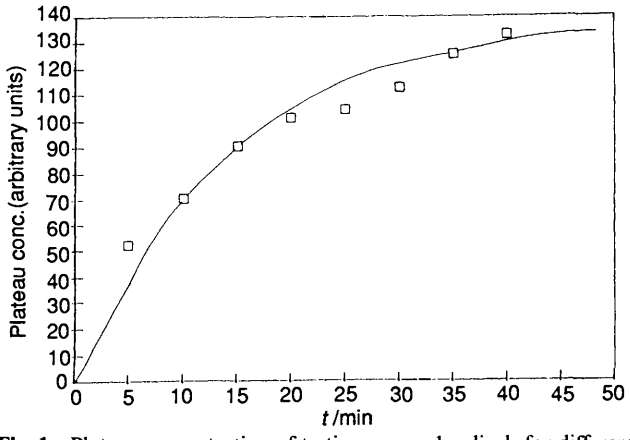

Fig. 1 Plateau concentration of tertiary peroxyl radicals for different photolysis times of azoisobutane (5×10^{-2} mol dm^{-3})/sisulfide (10^{-2} mol dm^{-3}) solutions at 218 K

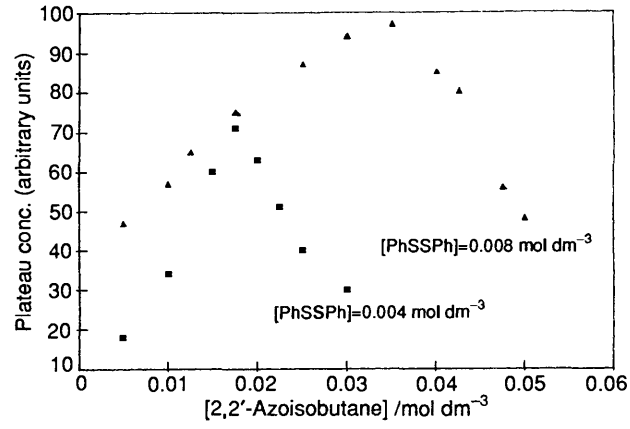

Fig. 2 Effects of azoisobutane (5×10^{-2}–5×10^{-3} mol dm^{-3}) and disulfide (4×10^{-3}–8×10^{-3} mol dm^{-3}) concentration on the plateau concentration of tertiary peroxyl radicals following photolysis at 218 K

in the regrowth at a particular AIB concentration (Fig. 2). Doubling the disulfide concentration, for example, led to a maximum at double the AIB concentration. The regrowth was always greater when the disulfide concentration was larger. We interpret these results as follows.

Consider the following termination reactions occurring during photolysis:

$$R'O_2^{\bullet} + R'O_2^{\bullet} \xrightarrow{k_7} R'OOR' + O_2$$

$$RS^{\bullet} + RS^{\bullet} \xrightarrow{k_8} RSSR$$

$$RS^{\bullet} + R'O_2^{\bullet} \xrightarrow{k_2} RSO_2R'$$

Then

$$\frac{[R'OOR'] + [R'SSR]}{[R'O_2SR]} = \frac{k_7[R'O_2^{\bullet}]^2 + k_8[RS^{\bullet}]^2}{k_2[RS^{\bullet}][R'O_2^{\bullet}]}$$

$$= \frac{k_7}{k_2} \times \frac{1}{f} + \frac{k_8}{k_2} \times f$$

where $f = \dfrac{[RS^{\bullet}]}{[R'O_2^{\bullet}]}$

Differentiating with respect to f gives

$$d\left[\frac{[R'OOR'] + [RSSR]}{[R'O_2SR]}\right]/df = \frac{-k_7}{k_2} f^{-2} + \frac{k_8}{k_2}$$

which will be zero at the minimum value of ([ROOR] + [RSSR])/[RO$_2$SR]. Thus the maximum RSO$_2$R yield will occur when

$$\frac{-k_7}{k_2} f^{-2} + \frac{k_8}{k_2} = 0$$

Rearranging gives

$$k_8[RS^{\bullet}]^2 = k_7[R'O_2^{\bullet}]^2$$

This relationship, together with application of the steady state approximation to [RS$^{\bullet}$] and [RO$_2^{\bullet}$] during photolysis leads to the following requirement for maximum [RSO$_2$R].

$$\varphi_{AIB}\{1 - \exp(-\varepsilon_{AIB}[AIB]d)\} = \varphi_{ss}\{1 - \exp(-\varepsilon_{ss}[RSSR]d)\} \quad (1)$$

where φ_{AIB} and φ_{ss} are the quantum yields of Bu^t$^{\bullet}$ and RS$^{\bullet}$ radicals. ε_{AIB} and ε_{ss} the respective extinction coefficients of AIB and disulfide and d is the pathlength.

This equality requires that $\varepsilon_{AIB}[AIB] \propto \varepsilon_{ss}[RSSR]$ for maximum yields of RSO$_2$R. Thus, the optimum level of [AIB] for maximum RSO$_2$R yields will be proportional to [RSSR], *i.e.*, doubling [RSSR] will require a doubling of [AIB] as found experimentally (Fig. 2).

Spin-trapping Experiments.—5,5-Dimethyl-1-pyrroline *N*-oxide (DMPO) is an efficient spin trap for both oxygen- and sulfur-centred radicals.[10,11,24-26] From the mechanism proposed we would predict that both thiyl and peroxyl or alkoxyl spin adducts should be produced by adding DMPO during photolysis. Only peroxyl/alkoxyl adducts should be observed soon after photolysis is terminated, as most of the thiyl radicals will have been lost by a rapid self-termination reaction. Addition of an excess of DMPO to an oxygenated solution of AIB (5×10^{-2} mol dm^{-3}) and (PhS)$_2$ (5×10^{-3} mol dm^{-3}) at 218 K during photolysis did indeed result in the spectrum showing both thiyl and butoxyl spin adducts with characteristic nitrogen and hydrogen hyperfine coupling constants. The identity of the adducts was confirmed by photolysing separate solutions of DMPO–(PhS)$_2$ and DMPO–(Bu^{t}O)$_2$. Injection of cold DMPO after photolysis resulted in the observation of only the *tert*-butoxyl spin adduct, which accumulated for about 8 min before decaying. Addition of DMPO after photolysis to AIB solution at 218 K also gave the *tert*-butoxyl spin adduct, the initial concentration of which was higher than when disulfide was present. This adduct only accumulated for 1 min before decaying, with its final concentration being lower than when the disulfide was present. This accumulation is attributed to peroxyls arising from residual tetraoxide decomposition at this temperature[27] and residual peroxyls present in solution because of their slow self-termination.

The trapping of an oxygen-centred radical, the concentration of which grows for 8 min on the post-irradiation addition of DMPO agrees with our postulated mechanism involving the decomposition of an unstable sulfanylperoxide.

Unfortunately, it is not possible to decide unequivocally whether the spin adduct is that from a *tert*-butoxyl or *tert*-peroxyl species since the *tert*-peroxyl–DMPO adduct is unstable and rearranges to a butoxyl adduct. Sulfinyl radicals (RSO$^{\bullet}$) undergo a very slow reaction with spin traps[28,29] and

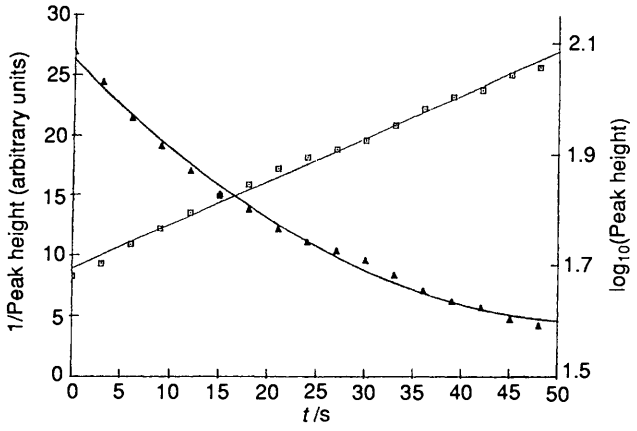

Fig. 3 First- and second-order plots for the decay of tertiary peroxyl radicals produced by photolysis of azoisobutane (5×10^{-2} mol dm^{-3}) at 214 K

are removed largely by rapid self-termination reactions, thus precluding their detection as spin adducts. No trace of a thiyl spin adduct was observed which suggests that the reverse of the sulfanylperoxyl-forming reaction does not occur to any marked extent.

Modelling.—Solutions of $(PhS)_2$ (10^{-2} mol dm^{-3}) and AIB (5×10^{-2} mol dm^{-3}) were photolysed for 5 min. On cessation of photolysis, the growth and subsequent decay of the peroxyl were recorded by taking multiple scans. These experiments were carried out in the temperature range 212–230 K, the temperature being restricted because below 208 K the disulfide precipitates out of solution and above 240 K there is the risk of decomposition of the trioxide Bu^{t}OOOBu^t, which may also be formed in these experiments. Also at higher temperatures the dissociation of the (*Z*)-2,2′-azoisobutane could occur and complicate the situation.

Similar experiments were carried out using $(Bu^tS)_2$ (10^{-1} mol dm^{-3}). A larger concentration of disulfide could be used because of its higher solubility, giving larger concentrations of thiyl radicals and hence more sulfanylperoxide product. Here, temperatures were kept in the range 177–202 K. Above 202 K decomposition of the sulfanylperoxide was too fast to be measured and below 173 K there is the problem of the tetraoxide–peroxide equilibrium.[27]

The decay characteristics of the peroxyl radicals were also investigated by photolysing oxygenated solutions of AIB in the temperature range 179–245 K, in order to circumvent problems arising from the *E*–*Z* isomerism of this alkyl radical source at lower temperatures. At all temperatures, the decay of the peroxyl radicals showed good second-order kinetic behaviour (Fig. 3), illustrating that the effect of the decomposition of the *Z*-isomer was negligible. The rate constant for the peroxyl termination was faster than previously reported[30] (see the Appendix).

Modelling of the growth and decay of the peroxyl (Scheme 1) during the 'dark' period was carried out by numerical integration of the appropriate differential rate equations,[31,32] with key parameters being varied until the observed concentration *vs.* time profile for peroxyl was reproduced. Initial estimates for insertion into the simulation routine were obtained by the following kinetic analysis.

The initial growth of peroxyls, assuming $k_3[RSOOR] \gg k_7[RO_2^{\bullet}]^2$, is given by eqn. (2).

$$\left[\frac{d[RO^{2\bullet}]}{dt}\right] = k_3[RSOOR]_0 = \alpha \qquad (2)$$

At the maximum concentration of peroxyls, time t_{max}

$$k_3[RSOOR]_{max} = k_7[RO_2^{\bullet}]_{max} = \beta \qquad (3)$$

At any time t,

$$[RSOOR]_t = [RSOOR]_0\exp(-k_3t) \qquad (4)$$

Now, substituting for $[RSOOR]_{t_{max}}$ into equation. (3)

$$k_3[RSOOR]_0\exp(-k_3t_{max}) = k_7[RO_2^{\bullet}]_{max} = \beta \qquad (5)$$

Substituting for α in eqn. (5),

$$\alpha\exp(-k_3t_{max}) = \beta$$

$$k_3 = \ln(\alpha/\beta)/t_{max} \qquad (6)$$

and $$[RSOOR]_0 = \alpha/k_3$$

Thus, from the initial slopes of the regrowth, the maximum peroxyl concentration and the experimentally determined termination rate constant of the peroxyl, estimates of k_3 and $[RSOOR]_0$ could be made and inserted as the initial starting parameters into the kinetic modelling algorithm. For instance, at 187 K, for Bu^{t}SOOBu^t decomposition values of $(RSOOR)_0 = 1.3 \times 10^{-6}$ mol dm^{-3} and $k_3 = 0.039$ s^{-1} were estimated in this way.

The total reaction scheme used in the modelling is brought together for convenience in Scheme 2.

$$R^tSOOR^t \xrightarrow{k_3} RSO^{\bullet} + R^tO^{\bullet} \qquad (7)$$

$$R^tO^{\bullet} + 2\text{-MB} \xrightarrow{k_4} R^{t\bullet} + ROH \qquad (8)$$

$$R^{t\bullet} + O_2 \xrightarrow{k_5} R^tO_2^{\bullet} \qquad (9)$$

$$R^tO_2^{\bullet} + R^tO_2^{\bullet} \xrightarrow{k_7} \text{non-radical products} \qquad (10)$$

$$R^tO^{\bullet} + R^tO_2^{\bullet} \xrightarrow{k_9} R^tO_3R^t \qquad (11)$$

$$R^tO^{\bullet} + R^tO^{\bullet} \xrightarrow{k_{10}} R^tOOR^t \qquad (12)$$

$$R^{t\bullet} + R^{t\bullet} \xrightarrow{k_{11}} R\text{–}R \qquad (13)$$

Scheme 2

The initial starting values for k_3 and $[RSOOR]_0$ were determined from eqns. (6). The literature values for k_4 and k_5 were employed.[22,23] An oxygen concentration of 10^{-3} mol dm^{-3} was used. The rate constant for reaction (10) was determined experimentally and found to be in the range *ca.* 10^3–10^4 for 179–245 K. Reactions (11)–(13) were assumed to be diffuson-controlled and a value of 10^8 was initially assigned to the rate constant of these reactions. The model was subsequently found to be insensitive to these reactions and the outcome was not affected if these reactions were omitted.

The kinetic curves were modelled to obtain the best fit by altering k_3 and the initial concentration of sulfanylperoxide, $[RSOOR]_0$. Once a good fit was obtained, the sensitivity of the model to k_3 was checked by altering its value together with $[RSOOR]_0$ so that the simulated concentration–time profiles of peroxyl matched the experimental. Typical comparisons of the computed and experimental curves about the best values of k_3 and $[RSOOR]_0$ are shown in Figs. 4 and 5. Visual

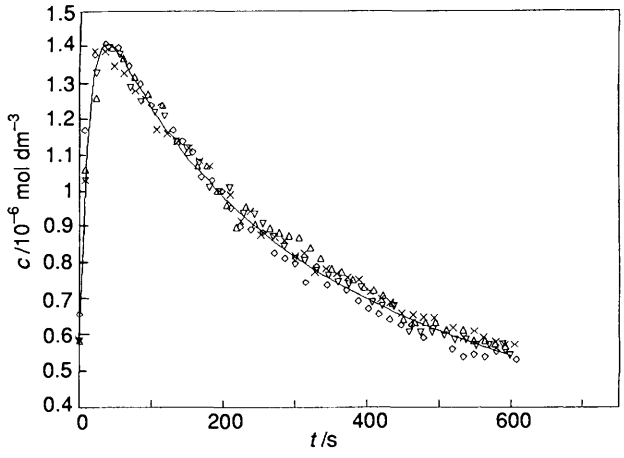

Fig. 4 Experimental data and computer simulation of the growth and decay of tertiary peroxyl radicals generated by the decomposition of Bu^{t}SOOBu^t at 202 K

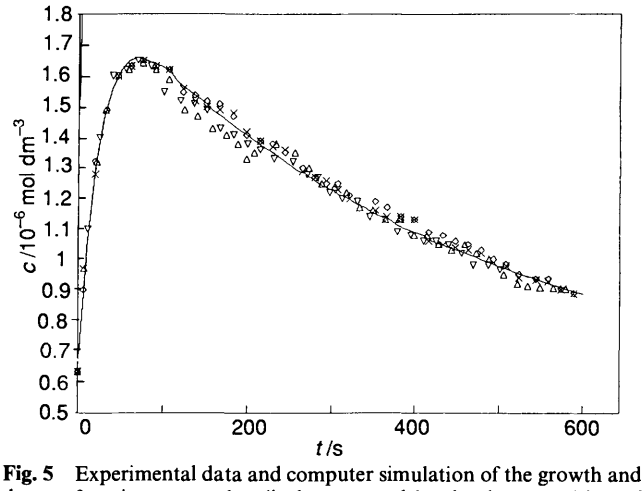

Fig. 5 Experimental data and computer simulation of the growth and decay of tertiary peroxyl radicals generated by the decomposition of Bu^{t}SOOBu^t at 187 K

examination of these curves indicates that only a narrow range of k_3 values reproduce the experimental observations and we estimate that variations of k_3 by about 10% are distinguishable. The experimental curves over a range of temperatures could be matched excellently with the algorithm and Scheme 2. The values of k_3 and $[RSOOR]_0$ which gave the best fit are given in Tables 1 and 2 and the Arrhenius parameters derived from Figs. 6 and 7 are listed in Table 3.

The Mechanism of Sulfanylperoxide (RSOOR) *Decomposition.*—Two aspects require particular discussion, namely (*a*) the low values of the *A* factors, and (*b*) the marked difference between the Arrhenius parameters of the phenyl and *tert*-butyl sulfanylperoxide decomposition.

Table 1 Values for Bu^{t}SOOBu^t decomposition (from the model)

T/K	$[Bu^tSOOBu^t]_0$/ mol dm^{-3}	k_3/s^{-1}
202	1×10^{-6}	0.08 ± 0.01
195	1.1×10^{-6}	0.055 ± 0.005
187	1.25×10^{-6}	0.04 ± 0.0025
177	1.5×10^{-6}	0.025 ± 0.0025

Table 2 Values for PhSOOBu^t decomposition (from the model)

T/K	$[PhSOOBu^t]_0$/ mol dm^{-3}	k_3/s^{-1}
230	3.65×10^{-7}	0.1 ± 0.02
225	3.9×10^{-7}	0.06 ± 0.01
218	4.2×10^{-7}	0.03 ± 0.005
212	4.6×10^{-7}	0.023 ± 0.007

Table 3 Arrhenius parameters for decomposition of the sulfanylperoxides

	Activation energy E_a/kJ mol^{-1}	$\log_{10} A$
Bu^{t}SOOBu^t	14 ± 3	2.4 ± 1.3
PhSOOBu^t	34 ± 13	6.6 ± 3

The *A* factor for the decomposition of Bu^{t}SOOBu^t is very low but similar low factors have been reported for the decomposition of other polyoxygen molecules such as molozonides[34] and hydrotrioxides.[35] The largest possible experimental value for *A* is 10^4 s^{-1} based on the steepest line and largest intercept. We suggest that the low value arises from a combination of a complex series of cage reactions and cage escape, following the initial decomposition of the sulfanylperoxide through a tight four-membered cyclic transition state to form alkoxyl and sulfinyl in a solvent cage. Square brackets indicate a cage reaction.

The experimental rate constants for the Arrhenius parameters are composite

$$k_{exp} = k_d k_e / k_f + k_e$$

If $k_f \gg k_e$, then

$$k_{exp} = \frac{k_d k_e}{k_f}$$

$$A_{exp} = \frac{A_d A_e}{A_f}, \quad E_{a(exp)} = E_d + E_e - E_f$$

A_e is a product of the collision frequency (*ca.* 10^{11} s^{-1}) between adjacent molecules in solution and a statistical factor

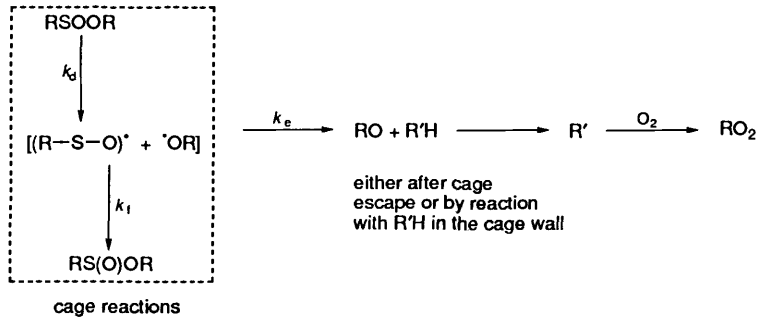

Scheme 3

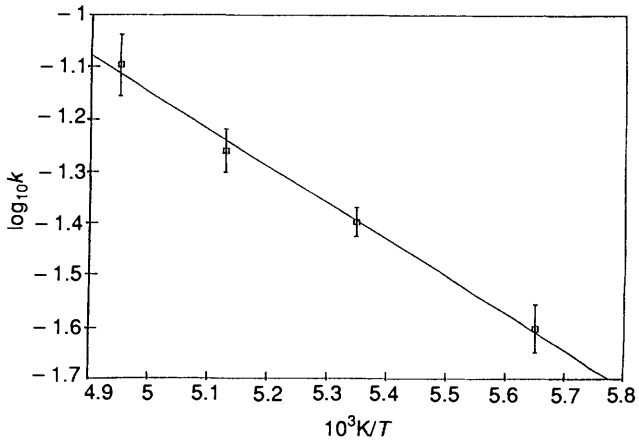

Fig. 6 Arrhenius plot for the decomposition of Bu'SOOBu'

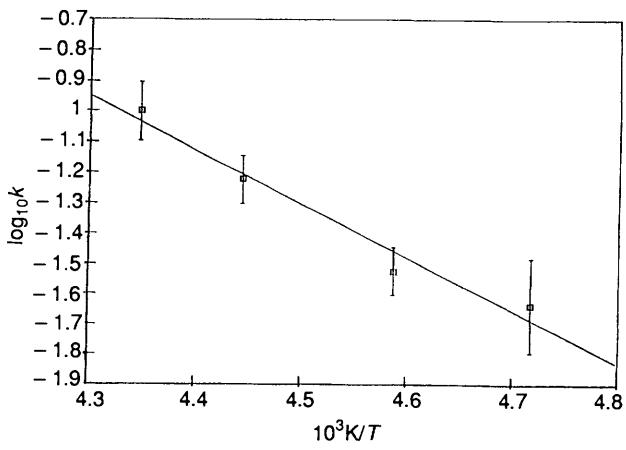

Fig. 7 Arrhenius plot for the decomposition of PhSOOBu'

either for reaction with 2-MB (*ca.* 10^{-3}) in the cage walls or escape through the cage walls. A_f will be close to 10^{11} s^{-1} and hence A_e/A_f will be approximately 10^{-3}. $A_d = \nu \exp(-\Delta S^{\ddagger}/R) = 10^{11} \exp(-\Delta S^{\ddagger}/R)$ where $\Delta S^{\ddagger}$ is the change in entropy in forming the transition state and ν is the encounter frequency $\approx 10^{11}$. There has to be an entropy loss of $\Delta S = -77$ to -145 J mol^{-1} K^{-1} for $A_{exp} = 10^{2.4}$ and 10^4, respectively, in the dissociation. The driving force for the dissociation is the formation of 'stable' sulfinyl radicals with a double bond between sulfur and oxygen and considerable delocalisation of the spin between these two centres in a SOMO with contributions from a π^* antibonding orbital or the empty 3d orbitals of sulfur. The EPR spectra of matrix isolated ^{33}S sulfinyls indicate 72–90% spin density at sulfur.[36,37] We suggest that double-bond formation is well advanced in the transition state which we envisage to have a rigid four-membered cyclic ring structure (Scheme 4). There will be loss of vibrational entropy (-24 to -32 J mol^{-1} K^{-1} for each normal mode)[38] on going from a single S–O to a double S=O bond and also a loss of entropy associated with loss of internal rotations around the developing S=O bond (approximately 30 J mol^{-1} K^{-1} for each internal rotation lost).[38,39] There will also be entropy losses associated with increasing solvent orientation at the increasing dipole of the S=O bond. Some measure of such losses can be obtained from the entropy of fussion of 2MB of 44 J mol^{-1} K^{-1}, indicating that considerable entropy loss could originate from this source.

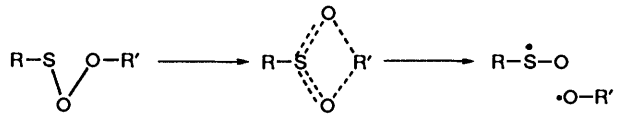

Scheme 4

Turning now to the difference between PhSOOBu' and Bu'SOOBu', we believe that this is most likely to be due to the occurrence of a different and concurrent mechanism, which is similar to that which is well established for phenolic inhibitors and peroxyl radicals.[40–42] Phenylthiyl, like phenoxyl, will possess considerable spin density at the *para* and *ortho* positions of the benzene ring. Peroxyl radicals can react by forming an O–C bond at these positions to form a 'normal' peroxide linkage in *tert*-butyl (4-thioxocyclohexa-2,5-dienyl) peroxide and *tert*-butyl (2-thioxocyclohexa-3,5-dienyl) peroxide for which we have coined the term peroxycyclohexadienethiones. This can either cleave directly to form a Bu'O$^{\bullet}$ radical and a thiocyclopentadienyloxyl radical or by reaction with O_2 to give Bu'O$^{\bullet}$,[43,44] $HO_2^{\bullet}$ and a *para*-thioquinone (Scheme 5). It is interesting to note that *para*-thioquinones[45] have been observed previously and *para*-quinones are well known products of peroxyl–phenoxyl reactions.[40]

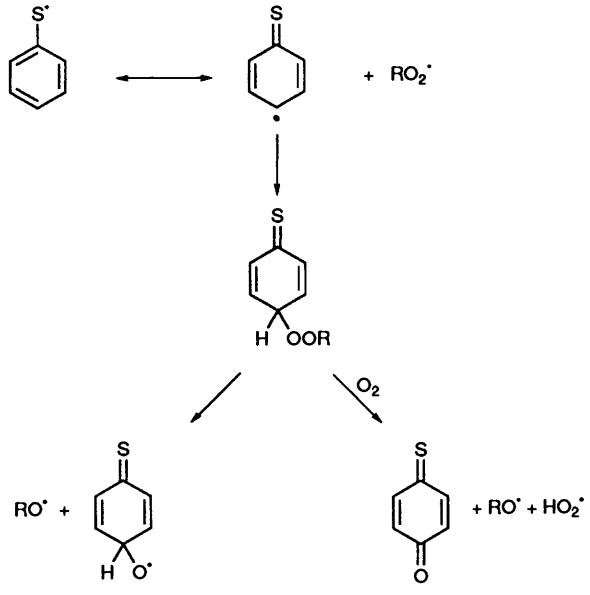

Scheme 5

The higher activation energy for PhSOOR decomposition is readily explicable because a peroxide bond (albeit one linked to a conjugated system) is being broken. If our suggestion is correct, then the strength of the sulfanylperoxide O–O bond is 36 kJ mol^{-1}, considerably weaker than similar bonds in phenolic analogues.

It is possible that the Arrhenius plot in Fig. 7 is curved. This might indicate that, at lower temperatures, the O–O bond cleavage with lower E_A and A factor predominates, while at higher temperatures the para O–O cleavage route becomes more important. Unfortunately, we cannot extend the temperature range sufficiently to rest this hypothesis further, but if we use the two higher temperature points we obtain $E_A = 44$ kJ mol^{-1} and $A = 10^9$ s^{-1}, while the lower temperature points give $E_A = 17$ kJ mol^{-1} and $A = 10^2$ s^{-1}. The latter value is close to those determined for Bu'SO–OBu' decomposition and, hence, lends some credence to this supposition.

There is a marked difference between the Arrhenius parameters for the di-*tert*-butyl sulfanylperoxide than for the di-*tert*-butyl trioxide,[13] $A = 10^{17}$ s^{-1}, activation energy = 96 kJ mol^{-1}. The substitution of one oxygen atom by a sulfur atom causes a sharp drop of 82 kJ mol^{-1} in activation energy because of the increased stability of the sulfinyls over peroxyls and the

development of a sulfur–oxygen double bond resulting in a tighter activated complex and a dramatic drop in A factor.

Appendix

The values used in the modelling for the termination of peroxyls are those determined in this work. The activation energy and A factors were found to be 14 kJ mol^{-1} and 8.9×10^6 compared with the previously calculated values of 35 kJ mol^{-1} and 1.5×10^{10} for a peroxide–hydroperoxide system. The effect of AIB on the rate of peroxyl self-termination was examined. It was observed that there was a linear relationship between the rate of peroxyl termination and the AIB concentration. The decay of peroxyl appears to be faster than previously measured because of the presence of AIB or an impurity therein. The AIB was obtained with a purity of 98% and, unfortunately, the impurities are unknown. Therefore at this stage, we are unable to distinguish whether the faster decay is due to AIB itself, being attacked by peroxyl at the N=N bond, or by an impurity.

References

1 L. Bateman and J. I. Cuneen, *J. Chem. Soc.*, 1955, 1596.
2 L. Bateman, M. Cain, T. Colclough and J. I. Cuneen, *J. Chem. Soc.*, 1962, 3570.
3 P. Koelewijn and H. Berger, *Recl. Trav. Chim. Pays-Bas*, 1972, **91**, 1275; 1974, **93**, 63.
4 W. J. M. van Tilborg and P. S. Smael, *Recl. Trav. Chim. Pays-Bas*, 1976, **95**, 38, 133.
5 J. R. Shelton, *Rubber Chem. Technol.*, 1974, **47**, 949.
6 A. J. Bridgewater and M. D. Sexton, *J. Chem. Soc., Perkin Trans. 2*, 1978, 530.
7 J. E. Bennett, G. Brunton, B. C. Gilbert and P. E. Whittall, *J. Chem. Soc., Perkin Trans. 2*, 1988, 1359.
8 B. C. Gilbert in *Sulfur-centred Radical Intermediates in Chemistry and Biology*, eds. C. Chatgilialoglu and K.-D. Asmus, Plenum, New York, 1990, p. 135.
9 C. von Sonntag in *Sulfur-centred Radical Intermediates in Chemistry and Biology*, eds. C. Chatgilialoglu and K.-D. Asmus, Plenum, New York, 1990, p. 39.
10 B. Mile, C. C. Rowlands, P. D. Sillman and M. J. Fildes, *J. Chem. Soc., Perkin Trans. 2*, 1992, 1431.
11 B. Mile, C. C. Rowlands, P. D. Sillman and M. J. Fildes, *J. Chem. Soc., Chem. Commun.*, 1992, 882.
12 P. D. Sillman, B. Mile, C. C. Rowlands and A. J. Holmes, unpublished results.
13 P. D. Bartlett and G. Guaraldi, *J. Am. Chem. Soc.*, 1967, **89**, 4799.
14 J. E. Bennett, G. Brunton and R. Summers, *J. Chem. Soc., Perkin Trans. 2*, 1980, 981.
15 K. Adamic, M. Dunn and K. U. Ingold, *Can. J. Chem.*, 1969, **47**, 287.
16 K. Adamic and K. U. Ingold, *Can. J. Chem.*, 1969, **47**, 295.
17 K. Adamic, D. F. Bowman and K. U. Ingold, *J. Am. Oil. Chem. Soc.*, 1970, **47**, 110.
18 T. Mill and R. S. Stringham, *Tetrahedron Lett.*, 1969, 1853.
19 J. E. Bennett, J. A. Eyre, C. P. Rimmer and R. Summers, *Chem. Phys. Lett.*, 1974, **26**, 69.
20 P. S. Engel and D. J. Bishop, *J. Am. Chem. Soc.*, 1975, **97**, 6754.
21 C. J. Durham, L. Glover and H. S. Mosher, *J. Am. Chem. Soc.*, 1960, **82**, 1508.
22 J. K. Kochi, *Free Radicals*, Wiley Interscience, London, 1973, vol. 1, p. 15.
23 J. E. Bennett, G. Brunton, B. C. Gilbert and P. E. Whitall, *J. Chem. Soc., Perkin Trans. 2*, 1988, 1359.
24 M. J. Davies, L. G. Forni and S. L. Shuker, *Chem. Biol. Interact.*, 1987, **61**, 177.
25 P. D. Josephy, D. Rehorek and E. G. Janzen, *Tetrahedron Lett.*, 1984, **28**, 1685.
26 C. Anderson-Evans, *Aldrichim. Acta*, 1979, 12.
27 J. E. Bennett, D. M. Brown and B. Mile, *Trans. Faraday Soc.*, 1970, **66**, 397.
28 Personal communication from Shell Research Ltd.
29 B. C. Gilbert and B. Gill, *J. Chem. Soc., Chem. Commun.*, 1978, 78.
30 Landolt-Bornstein, *Data and Functional Relationships in Science and Technology*, New series, Group: Atomic and Molecular Physics, ed. H. Fischer, Springer-Verlag, Berlin, 1984, **13**, p. 207.
31 A. Prothero and A. Robinson, *Math. Comp.*, 1974, **28**, 125.
32 A. Jones, *RSC. Specialist Periodical Report on Chemical Kinetics*, 1975, 1.
33 N. M. Emanual, E. T. Denisov, Z. K. Maizus, *Liquid-phase Oxidation of Hydrocarbons*, Plenum, New York, 1967.
34 B. Mile, G. Morris and B. Allcock, *J. Chem. Soc., Perkin Trans. 2*, 1979, 1644.
35 F. E. Story, D. E. Emge and R. W. Murray, *J. Am. Chem. Soc.*, 1976, **98**, 1880.
36 K. Nishikida and F. Williams, *J. Am. Chem. Soc.*, 1974, **96**, 4781.
37 C. Chatgilialoglu in *Chemistry of Sulfones and Sulfoxides*, eds. S. Patai, Z. Rappoport and C. J. M. Stirling, Wiley, Chichester, UK, 1988, p. 1081.
38 S. W. Benson, *Thermochemical Kinetics*, 3rd edn., Wiley, New York, 1990.
39 G. Nickless, *Inorganic Sulfur Chemistry*, Elsevier, 1968.
40 E. C. Horswill and K. U. Ingold, *Can. J. Chem.*, 1966, **44**, 263.
41 J. A. Howard, *Rubber Chem. Technol.*, 1974, **47**, 976.
42 E. T. Denisov, I. V. Khudyakov, *Chem. Rev.*, 1987, **87**, 1313.
43 D. E. Hoare and P. A. Whytock, *Can. J. Chem.*, 1967, **45**, 865.
44 W. G. Alcock and B. Mile, *Combust. Flame*, 1977, **29**, 133.
45 H. Bock, S. Mohmand, T. Hirabayashi, G. Maier, H. P. Reisenauer, *Chem. Ber.*, 1983, **116**, 273.

Paper 3/01958F